

Microwave to optical conversion with atoms on a superconducting chip

David Petrosyan,^{1,2,3} Klaus Mølmer,² József Fortágh,³ and Mark Saffman⁴

¹*Institute of Electronic Structure and Laser, FORTH, GR-71110 Heraklion, Crete, Greece*

²*Department of Physics and Astronomy, Aarhus University, DK-8000 Aarhus C, Denmark*

³*Physikalisches Institut, Eberhard Karls Universität Tübingen, D-72076 Tübingen, Germany*

⁴*Department of Physics, University of Wisconsin-Madison, Madison, Wisconsin 53706, USA*

(Dated: April 22, 2019)

We describe a scheme to coherently convert a microwave photon of a superconducting co-planar waveguide resonator to an optical photon emitted into a well-defined temporal and spatial mode. The conversion is realized by a cold atomic ensemble trapped above the surface of the superconducting atom chip, near the antinode of the microwave cavity. The microwave photon couples to a strong Rydberg transition of the atoms that are also driven by a pair of laser fields with appropriate frequencies and wavevectors for an efficient wave-mixing process. With only few thousand atoms in an ensemble of moderate density, the microwave photon can be completely converted into an optical photon emitted with high probability into the phase matched direction and, e.g., fed into a fiber waveguide. This scheme operates in a free-space configuration, without requiring strong coupling of the atoms to a resonant optical cavity.

I. INTRODUCTION

Superconducting quantum circuits, which operate in the microwave frequency range, are promising systems for quantum information processing [1, 2], as attested by the immense recent interest of academia and industry (e.g. Google, Microsoft, Intel, IBM, D-Wave Systems Inc., Rigetti Computing, Quantum Circuits Inc.). On the other hand, photons in the optical and telecommunication frequency range are the best and fastest carriers of quantum information over long distances [3, 4]. Hence there is an urgent need for efficient, coherent and reversible conversion between microwave and optical signals at the single quantum level [5]. Here we describe such a scheme, which is compatible with both superconducting quantum information processing and optical quantum communication technologies.

Previous work on the microwave to optical conversion includes studies of optically active dopants in solids [6, 7], as well as electro-optical [8] and opto-mechanical [9] systems. Cold atomic systems, however, have unique advantages over the other approaches. Atomic (spin) ensembles can couple to superconducting microwave resonators to realize quantum memory in the long-lived hyperfine manifold of levels [10, 11]. Using stimulated Raman techniques [12, 13], such spin-wave excitations stored in the hyperfine transition can be reversibly converted into optical photons. Here we propose and analyze an efficient wave-mixing scheme for microwave to optical conversion on a superconducting atom chip. Our scheme employs a Rydberg transition between the atomic states that strongly couple to a microwave coplanar waveguide resonator [14–17]. The resonator can also contain superconducting qubits, and hence our scheme can serve to interface them with optical photons.

We note a related work [18] on microwave to optical conversion using free-space six-wave mixing involving Rydberg states. The achieved photon conversion efficiency was, however, low, as only a small portion of the free-

space microwave field can interact with the active atomic medium. A microwave to optical conversion scheme using a single (Cs) atom that interacts with a superconducting microwave resonator on the Rydberg transition and with an optical cavity on an optical transition was discussed in [19]. The advantage of the single atom approach is that it requires moderate laser power for atom trapping and leads to less light scattering and perturbation of the superconducting resonator. It relies, however, on the technically demanding strong coupling of the single atom to both microwave and optical cavities. In contrast, our present approach uses a large ensemble of atoms with collectively enhanced coupling to the microwave cavity and it leads to a coherent, directional emission of the optical photon even without an optical cavity.

II. THE SYSTEM

Consider the system shown schematically in Fig. 1. An integrated superconducting atom chip incorporates a microwave resonator, possibly containing superconducting qubits, and wires for magnetic trapping of the atoms. An ensemble of $N \gg 1$ cold atoms is trapped near the chip surface, close to the antinode of the microwave cavity field. The relevant states of the atoms are the ground state $|g\rangle$, a lower electronically excited state $|e\rangle$ and a pair of highly-excited Rydberg states $|i\rangle$ and $|s\rangle$ (see the inset of Fig. 1). A laser field of frequency ω_p couples the ground state $|g\rangle$ to the Rydberg state $|i\rangle$ with time-dependent Rabi frequency Ω_p and large detuning $\Delta_p \equiv \omega_p - \omega_{ig} \gg |\Omega_p|$. The atoms interact non-resonantly with the microwave cavity mode \hat{c} on the strong dipole-allowed transition between the Rydberg states $|i\rangle$ and $|s\rangle$. The corresponding coupling strength (vacuum Rabi frequency) $\eta = (\varphi_{si}/\hbar)\varepsilon_c u(\mathbf{r})$ is proportional to the dipole moment φ_{si} of the atomic transition, the field per photon ε_c in the cavity, and the cavity mode function $u(\mathbf{r})$ at the atomic position \mathbf{r} . The Rydberg

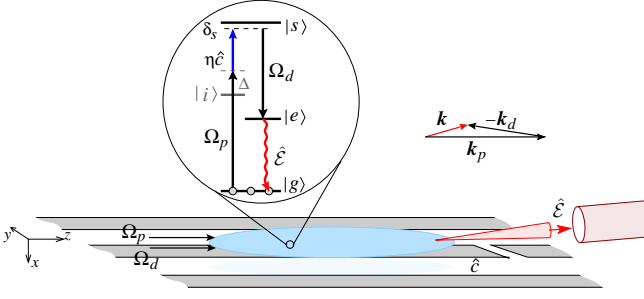


FIG. 1. Schematics of the system: An ensemble of atoms trapped on a superconducting chip near a coplanar waveguide cavity converts the microwave photon of the cavity to an optical photon fed into a fiber waveguide, as shown in the lower part of the figure. The inset shows the atomic level scheme. All the atoms are initially in the ground state $|g\rangle$. A laser pulse couples $|g\rangle$ to the intermediate Rydberg state $|i\rangle$ with the Rabi frequency Ω_p and detuning $\Delta_p \simeq \Delta$. The microwave cavity mode \hat{c} is coupled non-resonantly to the Rydberg transition $|i\rangle \rightarrow |s\rangle$ of the atoms with a position-dependent coupling strength η and detuning $\Delta_c \simeq -\Delta$. With large one-photon detunings $|\Delta_{p,c}| \gg |\Omega_p|, \eta$, the two-photon transition $|g\rangle \rightarrow |s\rangle$ to the Rydberg state $|s\rangle$ is detuned by $\delta_s = \Delta_p + \Delta_c$. A strong laser field Ω_d drives the transition from $|s\rangle$ to the electronically excited state $|e\rangle$ that rapidly decays with rate $\Gamma_e > \Omega_d$ to the ground state $|g\rangle$ and emits a photon \mathcal{E} predominantly into the phase-matched direction determined by the wave vector $\mathbf{k} = \mathbf{k}_p - \mathbf{k}_d$.

transition is detuned from the cavity mode resonance by $\Delta_c \equiv \omega_c - \omega_{si}$, $|\Delta_c| \gg \eta$. A strong driving field of frequency ω_d acts on the transition from the Rydberg state $|s\rangle$ to the lower excited state $|e\rangle$ with Rabi frequency Ω_d and detuning $\Delta_d = \omega_d - \omega_{se}$. The transition from excited state $|e\rangle$ to the ground state $|g\rangle$ is coupled with strengths $g_{\mathbf{k},\sigma}$ to the free-space quantized radiation field modes $\hat{a}_{\mathbf{k},\sigma}$ characterized by the wave vectors \mathbf{k} , polarization σ and frequencies $\omega_{\mathbf{k}} = ck$.

In the frame rotating with the frequencies of all the fields, ω_p , ω_c , ω_d , and $\omega_{\mathbf{k}}$, dropping for simplicity the polarization index, the Hamiltonian for the system reads

$$\begin{aligned} H/\hbar = & - \sum_{j=1}^N \left[\Delta_p^{(j)} \hat{\sigma}_{ii}^{(j)} + \delta_s^{(j)} \hat{\sigma}_{ss}^{(j)} + \delta_e \hat{\sigma}_{ee}^{(j)} \right. \\ & + \left(\Omega_p e^{i\mathbf{k}_p \cdot \mathbf{r}_j} \hat{\sigma}_{ig}^{(j)} - \eta(\mathbf{r}_j) \hat{c} \hat{\sigma}_{si}^{(j)} + \Omega_d e^{i\mathbf{k}_d \cdot \mathbf{r}_j} \hat{\sigma}_{se}^{(j)} \right. \\ & \left. \left. + \sum_{\mathbf{k}} g_{\mathbf{k}} \hat{a}_{\mathbf{k}} e^{i\mathbf{k} \cdot \mathbf{r}_j} e^{-i(\omega_{\mathbf{k}} - \omega_{eg})t} \hat{\sigma}_{eg}^{(j)} + \text{H.c.} \right) \right], \quad (1) \end{aligned}$$

where index j enumerates the atoms at positions \mathbf{r}_j , $\hat{\sigma}_{\mu\nu}^{(j)} \equiv |\mu\rangle_j \langle \nu|$ are the atomic projection ($\mu = \nu$) or transition ($\mu \neq \nu$) operators, \mathbf{k}_p and \mathbf{k}_d are the wave vectors of the corresponding laser fields, $\delta_s^{(j)} \equiv \Delta_p^{(j)} + \Delta_c^{(j)} = \omega_p + \omega_c - \omega_{sg}^{(j)}$ is the two-photon detuning of level $|s\rangle$, and $\delta_e \equiv \delta_s^{(j)} - \Delta_d^{(j)} = \omega_p + \omega_c - \omega_d - \omega_{eg}$ is the three-photon detuning of $|e\rangle$. The energies of the Rydberg levels $|i\rangle, |s\rangle$, and thereby the corresponding detunings $\Delta_{p,c}^{(j)}$

and $\delta_s^{(j)}$, depend on the atomic distance $(x_0 - x_j)$ from the chip surface at x_0 , which may contain atomic adsorbates producing an inhomogeneous electric field [20, 21]. We neglect the level shift of the lower state $|e\rangle$, since it is typically less sensitive to the electric fields and has a large width Γ_e (see below).

We assume that initially all the atoms are prepared in the ground state, $|G\rangle \equiv |g_1, g_2, \dots, g_N\rangle$, the microwave cavity contains a single photon, $|1_c\rangle$, and all the free-space optical modes are empty, $|0\rangle$. We can expand the state vector of the combined system as $|\Psi\rangle = b_0 |G\rangle \otimes |1_c\rangle \otimes |0\rangle + \sum_{j=1}^N d_j e^{i\mathbf{k}_p \cdot \mathbf{r}_j} |i_j\rangle \otimes |1_c\rangle \otimes |0\rangle + \sum_{j=1}^N c_j e^{i\mathbf{k}_p \cdot \mathbf{r}_j} |s_j\rangle \otimes |0_c\rangle \otimes |0\rangle + \sum_{j=1}^N b_j e^{i(\mathbf{k}_p - \mathbf{k}_d) \cdot \mathbf{r}_j} |e_j\rangle \otimes |0_c\rangle \otimes |0\rangle + |G\rangle \otimes |0_c\rangle \otimes \sum_{\mathbf{k}} a_{\mathbf{k}} |1_{\mathbf{k}}\rangle$, where $|\mu_j\rangle \equiv |g_1, g_2, \dots, \mu_j, \dots, g_N\rangle$ denote the single excitation states, $\mu = i, s, e$, and $|1_{\mathbf{k}}\rangle \equiv \hat{a}_{\mathbf{k}}^\dagger |0\rangle$ denotes the state of the radiation field with one photon in mode \mathbf{k} . The evolution of the state vector is governed by the Schrödinger equation $\partial_t |\Psi\rangle = -\frac{i}{\hbar} H |\Psi\rangle$ with the Hamiltonian (1), which leads to the system of coupled equations for the slowly-varying in space atomic amplitudes,

$$\partial_t b_0 = i \sum_{j=1}^N \Omega_p^* d_j, \quad (2a)$$

$$\partial_t d_j = i \Delta_p^{(j)} d_j + i \Omega_p b_0 - i \eta^*(\mathbf{r}_j) c_j, \quad (2b)$$

$$\partial_t c_j = i \delta_s^{(j)} c_j - i \eta(\mathbf{r}_j) d_j + i \Omega_d b_j, \quad (2c)$$

$$\begin{aligned} \partial_t b_j = & i \delta_e b_j + i \Omega_d^* c_j \\ & + i \sum_{\mathbf{k}} g_{\mathbf{k}} e^{i(\mathbf{k} - \mathbf{k}_p + \mathbf{k}_d) \cdot \mathbf{r}_j} a_{\mathbf{k}} e^{-i(\omega_{\mathbf{k}} - \omega_{eg})t}, \quad (2d) \end{aligned}$$

while the equation for the optical photon amplitudes written in the integral form is

$$a_{\mathbf{k}}(t) = i g_{\mathbf{k}}^* \sum_j e^{i(\mathbf{k}_p - \mathbf{k}_d - \mathbf{k}) \cdot \mathbf{r}_j} \int_0^t dt' b_j(t') e^{i(\omega_{\mathbf{k}} - \omega_{eg})t'}. \quad (3)$$

The initial conditions for Eqs. (2), (3) are $b_0(0) = 1$, $b_j(0), c_j(0), d_j(0) = 0 \forall j$, and $a_{\mathbf{k}}(0) = 0 \forall \mathbf{k}$.

We substitute Eq. (3) into the equation for atomic amplitudes b_j , assuming they vary slowly in time, and obtain the usual spontaneous decay of the atomic state $|e\rangle$ with rate Γ_e and the Lamb shift that can be incorporated into ω_{eg} [22]. We neglect the field-mediated interactions (multiple scattering) between the atoms [23–25], assuming random atomic positions and sufficiently large mean interatomic distance $\bar{r}_{ij} \gtrsim \lambda/2\pi$. To avoid the atomic excitation in the absence of a microwave photon in the cavity, we assume that the intermediate Rydberg level $|i\rangle$ is strongly detuned, $\Delta_p^{(j)} \simeq -\Delta_c^{(j)} \gg |\Omega_p|, \eta, |\delta_s^{(j)}|$ for all atoms in the ensemble. In addition, we assume that the variation of $\Delta_p^{(j)}$ ($\Delta_c^{(j)}$) across the atomic cloud is small compared to its mean value Δ ($-\Delta$), which presumes small enough Rydberg levels shifts in the inhomogeneous electric field. We can then adiabatically eliminate the

intermediate Rydberg level $|i\rangle$, obtaining finally

$$\partial_t b_0 = i \sum_{j=1}^N \tilde{\eta}_j c_j, \quad (4a)$$

$$\partial_t c_j = (i\tilde{\delta}_s^{(j)} - \Gamma_s/2)c_j + i\tilde{\eta}_j b_0 + i\Omega_d b_j, \quad (4b)$$

$$\partial_t b_j = (i\tilde{\delta}_e - \Gamma_e/2)b_j + i\Omega_d^* c_j, \quad (4c)$$

where $\tilde{\eta}_j \equiv \frac{\eta(\mathbf{r}_j)\Omega_p}{\Delta} [1 + \frac{\delta_s^{(j)}}{2\Delta}]$ is the second-order coupling between $|g_j\rangle \otimes |1_c\rangle$ and $|s_j\rangle \otimes |0_c\rangle$, while the second-order level shifts of $|g_j\rangle$ and $|s_j\rangle$ are incorporated into the detunings $\tilde{\delta}_s^{(j)} \equiv \delta_s^{(j)} + \frac{|\Omega_p|^2 - |\eta(\mathbf{r}_j)|^2}{\Delta}$ and $\tilde{\delta}_e = \delta_e + \frac{|\Omega_p|^2}{\Delta}$. We have also included the typically slow decay Γ_s of state $|s\rangle$ corresponding to the loss of Rydberg atoms [16, 26].

Before presenting the results of numerical simulations, we can derive an approximate analytic solution of the above equations and discuss its implications. We take a time-dependent pump field $\Omega_p(t)$ (and thereby $\tilde{\eta}_j(t)$) and a constant driving field $\Omega_d < \Gamma_e/2$, which results in an effective broadening of the Rydberg state $|s\rangle$ by $\gamma = \frac{|\Omega_d|^2}{\Gamma_e/2}$. Assuming $\gamma \gg \Gamma_s/2, \tilde{\delta}_e$, we then obtain

$$b_j(t) = -\frac{\gamma}{\Omega_d} \frac{\tilde{\eta}_j(t)}{\gamma - i\tilde{\delta}_s^{(j)}} b_0(t), \quad (5a)$$

$$b_0(t) = b_0(0) \exp \left[-\int_0^t dt' \sum_{j=1}^N \frac{|\tilde{\eta}_j(t')|^2}{\gamma - i\tilde{\delta}_s^{(j)}} \right]. \quad (5b)$$

Substituting these into Eq. (3) and separating the temporal and spatial dependence, we obtain

$$a_{\mathbf{k}}(t) = -i \frac{\gamma}{\Omega_d} A_{\mathbf{k}}(t) \times B_{\mathbf{k}}, \quad (6)$$

where

$$A_{\mathbf{k}}(t) = \int_0^t dt' \Omega_p(t') e^{i(\omega_{\mathbf{k}} - \omega_{eg})t'} e^{-\beta \int_0^{t'} dt'' |\Omega_p(t'')|^2}, \quad (7a)$$

$$B_{\mathbf{k}} = \frac{g_{\mathbf{k}}^*}{\Delta} \sum_{j=1}^N \frac{\eta(\mathbf{r}_j)}{\gamma - i\tilde{\delta}_s^{(j)}} e^{i(\mathbf{k}_p - \mathbf{k}_d - \mathbf{k}) \cdot \mathbf{r}_j}, \quad (7b)$$

with $\beta = \frac{1}{\Delta^2} \sum_{j=1}^N \frac{|\eta(\mathbf{r}_j)|^2}{\gamma - i\tilde{\delta}_s^{(j)}}$.

Equation (7a) shows that for a sufficiently smooth envelope of the pump field $\Omega_p(t)$, the optical photon is emitted within a narrow bandwidth $\beta|\Omega_p|^2$ around frequency $\omega_{\mathbf{k}} = \omega_{eg}$, which is a manifestation of the energy conservation. The temporal profile of the photon field at this frequency is $\epsilon(t) = \partial_t A_{\mathbf{k}_0}(t) = \Omega_p(t) e^{-\beta \int_0^t dt'' |\Omega_p(t'')|^2}$, where $k_0 = \omega_{eg}/c$. The envelope of the emitted radiation can be tailored to the desired profile $\epsilon(t)$ by shaping the pump pulse according to $\Omega_p(t) = \epsilon(t) [1 - 2\beta \int_0^t dt' |\epsilon(t')|^2]^{-1/2}$ [27], which can facilitate the photon transmission and its coherent re-absorption in a reverse process at a distant location [28–30]. Neglecting the photon dispersion during the propagation from the sending to the receiving node, and assuming the same or similar

physical setup at the receiving node containing an atomic ensemble driven by a constant field Ω_d , the complete conversion of the incoming optical photon to the cavity microwave photon is achieved by using the receiving laser pulse of the shape $\Omega_p(t) = -\epsilon(t) [2\beta \int_0^t dt' |\epsilon(t')|^2]^{-1/2}$ [27].

The spatial profile of the emitted radiation in Eq. (7b) is determined by the geometry of the atomic cloud, the excitation amplitudes of the atoms at different positions, and the phase matching. We assume an atomic cloud with normal density distribution $\rho(\mathbf{r}) = \rho_0 e^{-x^2/2\sigma_x^2 - y^2/2\sigma_y^2 - z^2/2\sigma_z^2}$ in an elongated harmonic trap, $\sigma_z > \sigma_{x,y}$. To maximize the resonant emission at frequency $\omega_{k_0} = c|\mathbf{k}_p - \mathbf{k}_d| = \omega_{eg}$ into the phase matched direction $\mathbf{k} = \mathbf{k}_p - \mathbf{k}_d$, we assume the (nearly) collinear geometry $\mathbf{k}_p, \mathbf{k}_d \parallel \mathbf{e}_z$. In an ideal case of all the atoms having the same excitation amplitude $b_j \propto 1/\sqrt{N} \forall j$, and hence $B_{\mathbf{k}} \propto \int d^3r \rho(\mathbf{r}) e^{i(\mathbf{k}_p - \mathbf{k}_d - \mathbf{k}) \cdot \mathbf{r}}$, the photon would be emitted predominantly into an (elliptic) Gaussian mode $\mathcal{E}(\mathbf{r}) \propto \sum_{|\mathbf{k}|=k_0} B_{\mathbf{k}} e^{i\mathbf{k} \cdot \mathbf{r}}$ with the waists $w_{0x,0y} = 2\sigma_{x,y}$, namely

$$\mathcal{E}(x, y, z) = \left(\frac{2}{\pi w_x w_y} \right)^{1/2} e^{ik_0(z + x^2/2q_x^* + y^2/2q_y^*)}, \quad (8)$$

where $w_{x,y} = w_{0x,0y} [1 + (\frac{z}{\zeta_{x,y}})^2]^{1/2}$ and $q_{x,y} = z + i\zeta_{x,y}$ with $\zeta_{x,y} = \frac{\pi w_{0x,0y}^2}{\lambda_0}$. The corresponding angular spread (divergence) of the beam is $\Delta\theta_{x,y} = \frac{\lambda_0}{\pi w_{0x,0y}} = \frac{1}{k_0 \sigma_{x,y}}$, which spans the solid angle $\Delta\Omega = \pi \Delta\theta_x \Delta\theta_y$. The probability of the phase-matched, cooperative photon emission into this solid angle is $P_{\Delta\Omega} \simeq \nu N \Delta\Omega$, while the probability of spontaneous, uncorrelated photon emission into a random direction is $P_{4\pi} \simeq \nu 4\pi$. With $P_{\Delta\Omega} + P_{4\pi} = 1$, we obtain $P_{\Delta\Omega} = \frac{N \Delta\Omega}{N \Delta\Omega + 4\pi}$ which approaches unity for $N \Delta\Omega \gg 4\pi$ or $N \gg 4k_0^2 \sigma_x \sigma_y$ [31]. Hence, for the product $N \Delta\Omega$, and thereby $P_{\Delta\Omega}$, to be large, we should take an elongated atomic cloud with large σ_z (to have many atoms N at a given atom density) and small σ_x, σ_y (to have large solid angle $\Delta\Omega$).

In our case, however, not all the atoms participate equally in the photon emission, since the atomic amplitudes $b_j \propto \frac{\eta(\mathbf{r}_j)}{\gamma - i\tilde{\delta}_s^{(j)}}$ depend strongly on the distance $(x_0 - x_j)$ from the chip surface via both the atom-cavity coupling strength $\eta(\mathbf{r}_j) \simeq \eta_0 e^{-(x_0 - x_j)/D}$, and, more sensitively, the Rydberg state detuning $\tilde{\delta}_s^{(j)} \simeq \alpha x_j$ (see below). This detuning results in a phase gradient for the atomic amplitudes in the x direction, which will lead to a small inclination of \mathbf{k} with respect to $\mathbf{k}_p - \mathbf{k}_d$ in the $x - z$ plane. More importantly, for strongly varying detuning, $\alpha > 2\gamma/\sigma_x$, only the atoms within a finite-width layer $\Delta x < \sigma_x$ are significantly excited to contribute to the photon emission. This reduces the cooperativity via $N \rightarrow \xi N$ with the effective participation fraction $\xi \simeq \frac{\Delta x}{\sigma_x} < 1$, but also leads to larger divergence $\Delta\theta_x \simeq \frac{1}{k_0 \Delta x}$ in the $x - z$ plane.

III. RESULTS

We have verified these arguments via exact numerical simulations of the dynamics of the system. We place N ground state $|g_j\rangle$ atoms in an elongated volume at random positions \mathbf{r}_j normally distributed around the origin, $x, y, z = 0$, with standard deviations $\sigma_z \gg \sigma_{x,y}$. With the peak density $\rho_0 = 2.35 \mu\text{m}^{-3}$ and $\sigma_{x,y} = 4 \mu\text{m}$, $\sigma_z = 24 \mu\text{m}$, we have $N = 15000$ atoms in the trap interacting with the co-planar waveguide resonator at position $x_0 \simeq 40 \mu\text{m}$ (see Fig. 1). Taking the strip-line length $L = 1 \text{ cm}$ and the grounded electrodes at distance $D = 10 \mu\text{m}$, the effective cavity volume is $V_c \simeq \pi D^2 L$ [10] yielding the field per photon $\varepsilon_c = \sqrt{\hbar\omega_c/\varepsilon_0 V_c} \simeq 0.5 \text{ V/m}$ for the cavity mode with $\omega_c/2\pi \sim 12 \text{ GHz}$. The atomic cloud is near the antinode of the cavity field which falls off evanescently with the distance from the chip surface as $u(\mathbf{r}) \simeq e^{-(x_0-x)/D}$. We choose the Rydberg states $|i\rangle = 68P_{1/2}$ and $|s\rangle = 69S_{1/2}$ of Rb with the quantum defects $\delta_P = 2.6545$ and $\delta_S = 3.131$, leading to the transition frequency $\omega_{si}/2\pi \simeq 12.2 \text{ GHz}$ and dipole moment $\varphi_{si} \simeq 1500a_0e$. This results in the vacuum Rabi frequency $\eta(0)/2\pi \simeq 190 \text{ kHz}$ at the cloud center $\mathbf{r} = 0$. We take a sufficiently large intermediate state detuning $\Delta/2\pi \simeq 10 \text{ MHz}$, and time-dependent pump field $\Omega_p(t) = \Omega_0 \frac{1}{2} [1 + \text{erf}(\frac{t-t_0}{\sqrt{2}\sigma_t})]$ of duration $t_{\text{end}} \simeq 10 \mu\text{s}$ with $t_0 = t_{\text{end}}/3$, $\sigma_t = t_{\text{end}}/8$ and the peak value $\Omega_0/2\pi \simeq 200 \text{ kHz}$ (see Fig. 2(a)). The wavelength of the pump field is $\lambda_p \simeq 297 \text{ nm}$ corresponding to a single-photon transition from $|g\rangle = 5S_{1/2}$ to $|i\rangle$; alternatively, a three-photon transition via intermediate $5P_{1/2}$ and $6S_{1/2}$ states is possible. The two-photon detuning $\tilde{\delta}_s$ of the Rydberg level $|s\rangle$ is taken to be zero at the cloud center $\mathbf{r} = 0$ and it varies with the atomic position along the x axis as $\tilde{\delta}_s(x) = \alpha x$ with $\alpha = 2\pi \times 0.5 \text{ MHz } \mu\text{m}^{-1}$ due to the residual or uncompensated surface charges on the atom chip [32, 33]. The strong laser field with wavelength $\lambda_d = 480 \text{ nm}$ is driving the transition from the Rydberg state $|s\rangle$ to $|e\rangle = 5P_{3/2}$ with a constant Rabi frequency $\Omega_d/2\pi = 1 \text{ MHz}$. The decay rates of states $|s\rangle$ and $|e\rangle$ are $\Gamma_s/2\pi = 1.6 \text{ kHz}$ and $\Gamma_e/2\pi = 6.1 \text{ MHz}$.

In Fig. 2 we show the results of our numerical simulations of the dynamics of the system and compare them with the analytical solutions. In the inset of Fig. 2(b) we show the time dependence of the total population $p_e(t) = \sum_{j=1}^N |b_j(t)|^2$ of the atoms in the excited state $|e\rangle$. As atoms decay from state $|e\rangle$ to the ground state $|g\rangle$, they emit a photon with rate $\Gamma_e |b_j(t)|^2$. The spatial distribution of time-integrated photon emission probability (in any direction) $P(\mathbf{r}_j) = \Gamma_e \int_0^{t_{\text{end}}} |b_j(t)|^2 dt$ is shown in Fig. 2(c). This probability follows the Gaussian density profile of the atoms along the y and z directions, but in the x direction it is modified by an approximate Lorentzian factor $\frac{|\eta(x)|^2}{\gamma^2 + \delta_s^2(x)}$ (if we neglect the x dependence of $\eta(x)$) due to the position-dependent detuning $\delta_s(x)$. Only part of the radiation is coherently emitted into the phase-matched direction $\mathbf{k} = \mathbf{k}_p - \mathbf{k}_d$, with

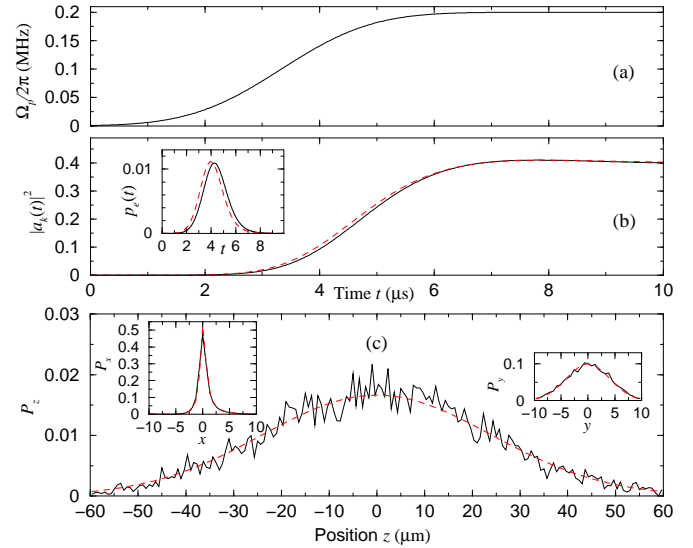


FIG. 2. (a) Rabi frequency of the pump field. (b) Probability $|a_{\mathbf{k}}(t)|^2$ (unnormalized) of photon emission into the resonant $\omega_{\mathbf{k}} = \omega_{eg}$, phase-matched $\mathbf{k} = \mathbf{k}_p - \mathbf{k}_d$ mode, obtained from the exact numerical (black solid line) and analytical (red dashed line) solutions. The inset shows the total population $p_e(t)$ of the atoms in state $|e\rangle$. (c) Spatial distribution of time-integrated photon emission probability (in any direction) P , as obtained from a single realization of the atomic ensemble. The main panel shows P_z along the z axis (integrated over the x and y direction), while the insets show P_x and P_y along x and y (black solid lines). For comparison, we show the Gaussians $P_z = \frac{1}{\sqrt{2\pi}\sigma_z} e^{-z^2/2\sigma_z^2}$ and $P_y = \frac{1}{\sqrt{2\pi}\sigma_y} e^{-y^2/2\sigma_y^2}$ for the z and y directions, and $P_x = \frac{1}{\mathcal{N}} \frac{|\eta(x)|^2}{\gamma^2 + \delta_s^2(x)} e^{-x^2/2\sigma_x^2}$ along x , with \mathcal{N} the normalization (red dashed lines).

probability $|a_{\mathbf{k}}(t)|^2$ of photon emission into the resonant $\omega_{\mathbf{k}} = \omega_{eg}$ mode shown in Fig. 2(b). Note that for non-resonant modes $\omega_{\mathbf{k}} \neq \omega_{eg}$ with the rapidly oscillating phase factor $e^{i(\omega_{\mathbf{k}} - \omega_{eg})t'}$ in Eq. (3) or (7a), the photon amplitude $a_{\mathbf{k}}(t) \propto \sum_j b_j(t)$ tends to zero at large times t_{end} (as do $b_j(t)$'s), even for the phase-matched direction $\mathbf{k} \simeq \mathbf{k}_p - \mathbf{k}_d$.

In Fig. 3 we show the angular probability distribution of the emitted photon. The beam divergence $\Delta\theta_x = \frac{1}{k_0 \Delta x} \simeq 0.015\pi$ in the $x - z$ plane is almost twice larger than that $\Delta\theta_y = \frac{1}{k_0 \sigma_y} \simeq 0.008\pi$ in the $y - z$ plane, consistent with the narrower spatial distribution $\Delta x \simeq 2.6 \mu\text{m} < \sigma_x = 4 \mu\text{m}$ of the atomic excitation (or emission) probability $P(\mathbf{r})$, as discussed above. In the collinear geometry, $\mathbf{k}_p, \mathbf{k}_d \parallel \hat{z}$, the radiation is emitted at a small angle $\theta_{x0} = \mathbf{k} \angle \hat{z} \simeq 0.014\pi$ due to the detuning induced phase gradient of the atomic amplitudes b_j along x . With a small angle $\mathbf{k}_d \angle \mathbf{k}_p = 0.009\pi$ between the drive and the pump fields, the latter still propagating along z , we can compensate this phase gradient, resulting in the photon emission along z ($\theta_{x0} = 0$). We may approximate the angular profile of the emitted radiation with a

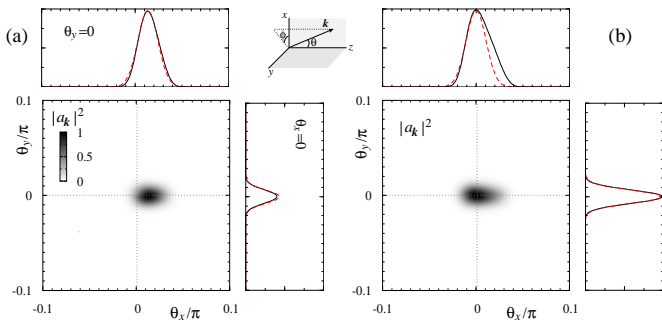


FIG. 3. Angular probability distribution $|a_{\mathbf{k}}|^2$ (unnormalized) of the photon emitted along the z direction, as a function of $\theta_x = \theta \cos(\phi)$ and $\theta_y = \theta \sin(\phi)$ with θ the polar and ϕ the azimuthal angles, as shown in middle top inset. Panel (a) corresponds to the case of the collinear geometry $\mathbf{k}_p, \mathbf{k}_d \parallel \hat{z}$, with the radiation emitted at a small angle $\theta_{x0} = \mathbf{k} \angle \hat{z} \simeq 0.014\pi$. Panel (b) shows the case with a small inclination $\mathbf{k}_d \angle \hat{z} = 0.009\pi$ and $\mathbf{k}_p \parallel \hat{z}$, leading to $\mathbf{k} \parallel \hat{z}$ ($\theta_{x0} = 0$). The red dashed lines in the insets of each density plot show the Gaussian $B(\theta_x, \theta_{x0}; \theta_y, \theta_{y0})$ of Eq. (9) with $\theta_y = 0$ (upper insets) and $\theta_x = 0$ (right insets), while $\theta_{y0} = 0$ and θ_{x0} as per cases (a) and (b).

Gaussian function

$$B_{\mathbf{k}} \propto B(\theta_x, \theta_{x0}; \theta_y, \theta_{y0}) = e^{-(\theta_x - \theta_{x0})^2 / \Delta\theta_x^2} e^{-(\theta_y - \theta_{y0})^2 / \Delta\theta_y^2}. \quad (9)$$

We then see from Fig. 3 that in the $y-z$ plane the angular profile corresponds to a Gaussian mode with $\theta_{y0} = 0$, but in the $x-z$ plane the angular profile deviates from the Gaussian, the more so for the case of the corrected emission angle $\theta_{x0} = 0$. To fully collect this radiation, we thus need to engineer an elliptic lens with appropriate non-circular curvature along the x direction.

The total probability of radiation emitted into the free-space spatial mode $\mathcal{E}(\mathbf{r})$ subtending the solid angle $\Delta\Omega = \pi\Delta\theta_x\Delta\theta_y$ is $P_{\Delta\Omega} \simeq 0.74$. This probability can be increased by optimizing the geometry of the sample, e.g., making it narrower and longer, as discussed above. Alternatively, we can enhance the collection efficiency of the coherently emitted radiation by surrounding the atoms by a moderate finesse, one-sided optical cavity. Assuming a resonant cavity with frequency ω_{k_0} , mode function $u_o(\mathbf{r})$ and length L_o , the overlap $v = \frac{1}{\sqrt{L_o}} \int d^3r \mathcal{E}(\mathbf{r}) u_o^*(\mathbf{r})$ determines the fraction of the radiation emitted by the atomic ensemble into the cavity mode, while the cavity finesse F determines the number of round trips of the radiation, $n \simeq F/2\pi$, and thereby the number of times it in-

teracts with the atoms, before it escapes the cavity. The probability of coherent emission of radiation by N atoms into the cavity output mode is then $P_{\text{out}} \simeq \frac{|v|^2 n N}{|v|^2 n N + 4\pi}$.

IV. CONCLUSIONS

We have proposed a scheme for coherent microwave to optical conversion of a photon of a superconducting resonator using an ensemble of atoms trapped on a superconducting atom chip. The converted optical photon with tailored temporal and spatial profiles can be fed into a waveguide and sent to a distant location, where the reverse process in a compatible physical setup can coherently convert it back into a microwave photon and, e.g., map it onto a superconducting qubit.

In our scheme, the atoms collectively interact with the microwave cavity via a strong, dipole-allowed Rydberg transition. We have considered the conversion of at most one microwave photon to an optical photon, for which the interatomic interactions and the resulting Rydberg excitation blockade [34, 35] do not play a role. In the case of multiple photons, however, the long-range interatomic interactions will induce strong non-linearities accompanied by the suppression of multiple Rydberg excitations within the blockade volume associated with each photon [36, 37]. This can potentially hinder the microwave photon conversion and optical photon collection due to distortion of the temporal and spatial profile of the emitted radiation. Our scheme, however, is primarily intended for communication between microwave operated quantum sub-registers and, as such, it should ideally deal with at most one microwave photon encoding a qubit state at a time. Yet, in the limit of a few photons interacting with many atoms in a volume much larger than the blockade volume, we expect the conversion to be well approximated as a linear process.

ACKNOWLEDGMENTS

We acknowledge support by the US ARL-CDQI program through cooperative agreement W911NF-15-2-0061, and by the DFG SPP 1929 GiRyd and DFG Project No. 394243350. D.P. is grateful to the Aarhus Institute of Advanced Studies for hospitality, and to the Alexander von Humboldt Foundation for additional support in the framework of the Research Group Linkage Programme.

-
- [1] J. Clarke and F.K. Wilhelm, *Superconducting quantum bits*, Nature **453**, 1031 (2008).
 [2] M. H. Devoret and R. J. Schoelkopf, *Superconducting Circuits for Quantum Information: An Outlook*, Science **339**, 1169 (2013).
 [3] H.J. Kimble, *The quantum internet*, Nature **453**, 1023

- (2008).
 [4] J. L. O'Brien, A. Furusawa and J. Vuckovic, *Photonic quantum technologies*, Nature Photon. **3**, 687 (2009).
 [5] G. Kurizki, P. Bertet, Y. Kubo, K. Mølmer, D. Petrosyan, P. Rabl, and J. Schmiedmayer, *Quantum technologies with hybrid systems*, PNAS **112**, 3866 (2015).

- [6] C. O'Brien, N. Lauk, S. Blum, G. Morigi, and M. Fleischhauer, *Interfacing Superconducting Qubits and Telecom Photons via a Rare-Earth-Doped Crystal*, Phys. Rev. Lett. **113**, 063603 (2014); S. Blum, C. O'Brien, N. Lauk, P. Bushev, M. Fleischhauer, and G. Morigi, *Interfacing microwave qubits and optical photons via spin ensembles*, Phys. Rev. A **91**, 033834 (2015).
- [7] L.A. Williamson, Y.-H. Chen, and J.J. Longdell, *Magneto-Optic Modulator with Unit Quantum Efficiency*, Phys. Rev. Lett. **113**, 203601 (2014).
- [8] A. Rueda, F. Sedlmeir, M.C. Collodo, U. Vogl, B. Stiller, G. Schunk, D. V. Strekalov, C. Marquardt, J. M. Fink, O. Painter, G. Leuchs, and H. G. L. Schwefel, *Efficient microwave to optical photon conversion: an electro-optical realization*, Optica **3**, 597 (2016).
- [9] R. W. Andrews, R. W. Peterson, T. P. Purdy, K. Cicak, R. W. Simmonds, C. A. Regal and K. W. Lehnert, *Bidirectional and efficient conversion between microwave and optical light*, Nature Phys. **10**, 321 (2014)
- [10] J. Verdu, H. Zoubi, Ch. Koller, J. Majer, H. Ritsch, and J. Schmiedmayer, *Strong Magnetic Coupling of an Ultracold Gas to a Superconducting Waveguide Cavity*, Phys. Rev. Lett. **103**, 043603 (2009).
- [11] H. Hattermann, D. Bothner, L. Y. Ley, B. Ferdinand, D. Wiedmaier, L. Sarkany, R. Kleiner, D. Koelle, and J. Fortagh, *Coupling ultracold atoms to a superconducting coplanar waveguide resonator*, Nat. Commun. **8**, 2254 (2017).
- [12] M. Fleischhauer, A. Imamoglu, and J. P. Marangos, *Electromagnetically induced transparency: Optics in coherent media*, Rev. Mod. Phys. **77**, 633 (2005).
- [13] K. Hammerer, A. S. Sørensen, and E. S. Polzik, *Quantum interface between light and atomic ensembles*, Rev. Mod. Phys. **82**, 1041 (2010).
- [14] D. Petrosyan, G. Bensky, G. Kurizki, I. Mazets, J. Majer and J. Schmiedmayer, *Reversible state transfer between superconducting qubits and atomic ensembles*, Phys. Rev. A **79**, 040304(R) (2009).
- [15] S. D. Hogan, J. A. Agner, F. Merkt, T. Thiele, S. Filipp, and A. Wallraff, *Driving Rydberg-Rydberg Transitions from a Coplanar Microwave Waveguide*, Phys. Rev. Lett. **108**, 063004 (2012).
- [16] C. Hermann-Avigliano, R. C. Teixeira, T. L. Nguyen, T. Cantat-Moltrecht, G. Nogues, I. Dotsenko, S. Gleyzes, J. M. Raimond, S. Haroche, and M. Brune, *Long coherence times for Rydberg qubits on a superconducting atom chip*, Phys. Rev. A **90**, 040502(R) (2014).
- [17] R. Celistrino Teixeira, C. Hermann-Avigliano, T. L. Nguyen, T. Cantat-Moltrecht, J. M. Raimond, S. Haroche, S. Gleyzes, and M. Brune, *Microwaves Probe Dipole Blockade and van der Waals Forces in a Cold Rydberg Gas*, Phys. Rev. Lett. **115**, 013001 (2015).
- [18] J. Han, T. Vogt, C. Gross, D. Jaksch, M. Kiffner, and W. Li, *Coherent Microwave-to-Optical Conversion via Six-Wave Mixing in Rydberg Atoms*, Phys. Rev. Lett. **120**, 093201 (2018); T. Vogt, C. Gross, J. Han, S. B. Pal, M. Lam, M. Kiffner, W. Li, *Efficient microwave-to-optical conversion using Rydberg atoms*, Phys. Rev. A **99**, 023832 (2019).
- [19] B. T. Gard, K. Jacobs, R. McDermott, and M. Saffman, *Microwave-to-optical frequency conversion using a cesium atom coupled to a superconducting resonator*, Phys. Rev. A **96**, 013833 (2017).
- [20] A. Tauschinsky, R. M. T. Thijssen, S. Whitlock, H. B. van Linden van den Heuvell, and R. J. C. Spreeuw, *Spatially resolved excitation of Rydberg atoms and surface effects on an atom chip*, Phys. Rev. A **81**, 063411 (2010).
- [21] H. Hattermann, M. Mack, F. Karlewski, F. Jessen, D. Cano, and J. Fortagh, *Detrimental adsorbate fields in experiments with cold Rydberg gases near surfaces*, Phys. Rev. A **86**, 022511 (2012).
- [22] M. O. Scully and M. S. Zubairy, *Quantum Optics* (Cambridge University Press, Cambridge, 1997).
- [23] R. H. Lehmann, *Radiation from an N-Atom System*, Phys. Rev. A **2**, 883 (1970); **2**, 889 (1970).
- [24] D.P. Craig and T. Thirunamachandran, *Molecular Quantum Electrodynamics* (Academic Press, London, 1984).
- [25] Y. Miroshnychenko, U. V. Poulsen, and K. Mølmer, *Directional emission of single photons from small atomic samples*, Phys. Rev. A **87**, 023821 (2013).
- [26] I. I. Beterov, I. I. Ryabtsev, D. B. Tretyakov, and V. M. Entin, *Quasiclassical calculations of blackbody-radiation-induced depopulation rates and effective lifetimes of Rydberg nS , nP , and nD alkali-metal atoms with $n \leq 80$* , Phys. Rev. A **79**, 052504 (2009); Erratum Phys. Rev. A **80**, 059902 (2009).
- [27] A. H. Kiilerich and K. Mølmer, *Input-Output Theory with Quantum Pulses*, arXiv:1902.09833.
- [28] J. McKeever, A. Boca, A.D. Boozer, R. Miller, J.R. Buck, A. Kuzmich, and H.J. Kimble, *Deterministic generation of single photons from one atom trapped in a cavity*, Science **303**, 1992 (2004).
- [29] M. Hijlkema, B. Weber, H. P. Specht, S. C. Webster, A. Kuhn and G. Rempe, *A single-photon server with just one atom*, Nature Phys. **3**, 253 (2007).
- [30] A. Reiserer and G. Rempe, *Cavity-based quantum networks with single atoms and optical photons*, Rev. Mod. Phys. **87**, 1379 (2015).
- [31] M. Saffman and T.G. Walker, *Entangling single- and N-atom qubits for fast quantum state detection and transmission*, Phys. Rev. A **72**, 042302 (2005).
- [32] J. A. Sedlacek, E. Kim, S. T. Rittenhouse, P. F. Weck, H. R. Sadeghpour, and J. P. Shaffer, *Electric Field Cancellation on Quartz by Rb Adsorbate-Induced Negative Electron Affinity*, Phys. Rev. Lett. **116**, 133201 (2016).
- [33] D. W. Booth, J. Isaacs, and M. Saffman, *Reducing the sensitivity of Rydberg atoms to dc electric fields using two-frequency ac field dressing*, Phys. Rev. A **97**, 012515 (2018).
- [34] M.D. Lukin, M. Fleischhauer, R. Côté, L.M. Duan, D. Jaksch, J.I. Cirac, and P. Zoller, *Dipole Blockade and Quantum Information Processing in Mesoscopic Atomic Ensembles*, Phys. Rev. Lett. **87**, 037901 (2001).
- [35] M. Saffman, T.G. Walker, and K. Mølmer, *Quantum information with Rydberg atoms*, Rev. Mod. Phys. **82**, 2313 (2010).
- [36] C. Murray and T. Pohl, *Quantum and nonlinear optics in strongly interacting atomic ensembles*, Adv. Atom. Mol. Opt. Phys. **65**, 321 (2016).
- [37] O. Firstenberg, C.S. Adams and S. Hofferberth, *Nonlinear quantum optics mediated by Rydberg interactions*, J. Phys. B **49**, 152003 (2016).